Received: 2 April 2018 | Revised: 2 July 2018 | Accepted: 12 July 2018

DOI: 10.1002/hbm.24326

WILEY

RESEARCH ARTICLE

Resting-state functional connectivity of subcortical locomotor centers explains variance in walking capacity

Pierce Boyne[1] | Thomas Maloney[2] | Mark DiFrancesco[2] | Michael D. Fox[3,4,5] | Oluwole Awosika[6] | Pushkar Aggarwal[1] | Jennifer Woeste[1] | Laurel Jaroch[1] | Daniel Braswell[1] | Jennifer Vannest[2]

[1]Department of Rehabilitation, Exercise and Nutrition Sciences, College of Allied Health Sciences, University of Cincinnati, Cincinnati, Ohio

[2]Pediatric Neuroimaging Research Consortium, Cincinnati Children's Hospital Medical Center, Cincinnati, Ohio

[3]Berenson-Allen Center for Noninvasive Brain Stimulation, Department of Neurology, Beth Israel Deaconess Medical Center, Harvard Medical School, Boston, Massachusetts

[4]Department of Neurology, Massachusetts General Hospital, Harvard Medical School, Boston, Massachusetts

[5]Athinoula A. Martinos Center for Biomedical Imaging, Harvard Medical School, Boston, Massachusetts

[6]Department of Neurology and Rehabilitation Medicine, College of Medicine, University of Cincinnati, Cincinnati, Ohio

Correspondence
Pierce Boyne, PT, DPT, PhD, NCS, Department of Rehabilitation, Exercise and Nutrition Sciences, College of Allied Health Sciences, University of Cincinnati, 3202 Eden Ave, Cincinnati, OH 45267.
Email: pierce.boyne@uc.edu

Funding information
American Heart Association, Grant/Award Number: 17MCPRP33670446; National Center for Advancing Translational Sciences, Grant/Award Number: KL2TR001426

Abstract

Walking capacity influences the quality of life and disability in normal aging and neurological disease, but the neural correlates remain unclear and subcortical locomotor regions identified in animals have been more challenging to assess in humans. Here we test whether resting-state functional MRI connectivity (rsFC) of midbrain and cerebellar locomotor regions (MLR and CLR) is associated with walking capacity among healthy adults. Using phenotypic and MRI data from the Nathan Kline Institute Rockland Sample (n =119, age 18–85), the association between walking capacity (6-min walk test distance) and rsFC was calculated from subcortical locomotor regions to 81 other gait-related regions of interest across the brain. Additional analyses assessed the independence and specificity of the results. Walking capacity was associated with higher rsFC between the MLR and superior frontal gyrus adjacent to the anterior cingulate cortex, higher rsFC between the MLR and paravermal cerebellum, and lower rsFC between the CLR and primary motor cortex foot area. These rsFC correlates were more strongly associated with walking capacity than phenotypic variables such as age, and together explained 25% of the variance in walking capacity. Results were specific to locomotor regions compared with the other brain regions. The rsFC of locomotor centers correlates with walking capacity among healthy adults. These locomotion-related biomarkers may prove useful in future work aimed at helping patients with reduced walking capacity.

KEYWORDS

brain, gait, locomotion, magnetic resonance imaging, network

1 | INTRODUCTION

Bipedal locomotion is a fundamental human function that underlies performance of many daily activities. Diminished walking capacity generally occurs during aging and is also a common consequence of brain disorders, including stroke, Parkinson's disease, traumatic brain injury, and Alzheimer's disease (Middleton, Fritz, & Lusardi, 2015). The decrease in walking function due to these conditions is associated with many negative sequelae, including functional dependence, frailty, cognitive decline, falls, institutionalization, hospitalization, low quality of life, decreased participation in life roles, depression, cardiovascular events, and death (Middleton et al., 2015). Therefore, improved walking capacity is often a primary goal of neurologic rehabilitation (Bohannon, Horton, & Wikholm, 1991; Winstein et al., 2016). However, optimal diagnosis, prognosis, and intervention for neurologic gait dysfunction will likely require a thorough understanding of how the

brain normally contributes to locomotion, and this area of research has proved challenging in humans.

Animal studies have consistently identified at least two subcortical centers that independently and synergistically generate locomotion when stimulated: the midbrain locomotor region (MLR) and the cerebellar locomotor region (CLR). The MLR is a functionally defined area including the pedunculopontine nucleus (PPN) and cuneiform nuclei (Mori, Matsuyama, Mori, & Nakajima, 2001; Takakusaki, 2013). The CLR is located in the antero-medial cerebellar white matter and is made up of efferent fibers from the fastigial nuclei (Mori et al., 2001; Takakusaki, 2013). Primary efferent projections from both the MLR and CLR converge on the pontomedulary reticular formation, where locomotor signals are sent to the spinal cord central pattern generators via the reticulospinal tracts (Mori et al., 2001; Takakusaki, 2013). The MLR receives diverse inputs from the premotor and primary motor cortices, limbic areas and cerebellum, as well as tonic inhibitory input from the basal ganglia (Alam, Schwabe, & Krauss, 2011; Jahn, Deutschlander, Stephan, Kalla, Hufner et al., 2008; Muthusamy et al., 2007; Takakusaki, 2013). The fastigial nuclei (which give rise to the CLR) receive inputs from the vermis and paravermal cerebellum; an area that integrates proprioceptive, vestibular, and visual information (Mori et al., 2001). This subcortically centered locomotor network appears to be largely responsible for automatic (unconscious) steady-state gait processes, presumably with prefrontal cortex and other limbic inputs contributing to gait motivation, initiation and sustainment (Figure 1; left). Cortical sensorimotor networks contribute to conscious gait control and higher level modifications in response to the environment, both via direct corticospinal/brainstem outputs and via feedback loops involving the basal ganglia and cerebellum (Figure 1; right; Bohnen & Jahn, 2013; Takakusaki, 2013).

The animal subcortical locomotor network also appears to have been largely preserved in humans. For example, imagined walking during functional MRI (task fMRI) and actual walking followed by positron emission tomography have each been shown to activate regions corresponding with the MLR and CLR in humans (la Fougere et al., 2010; Jahn, Deutschlander, Stephan, Kalla, Hufner et al., 2008; Jahn, Deutschlander, Stephan, Kalla, Wiesmann et al., 2008). In addition, electroencephalography and near-infrared regional spectroscopy studies have confirmed the involvement of primary motor and premotor cortical areas during actual human locomotion, in addition to other cortical regions (Gwin et al., 2011; Knaepen, Mierau, Tellez, Lefeber, & Meeusen, 2015; Miyai et al., 2001). However, these techniques are difficult to use for assessing gait neurophysiology because they lack subcortical definition, have low temporal resolution, require injection of a radioactive agent, are challenged by head motion during actual walking, and/or depend on the participant's motor imagery ability (Bohnen & Jahn, 2013).

Resting-state fMRI functional connectivity (rsFC) analysis may be a useful complement to these techniques for studying human locomotor control. This analysis method does not require task performance to obtain task-relevant physiologic signals, and it can be used to assess subcortical structures without exposure to ionizing radiation (Fox & Greicius, 2010). The rsFC approach is based on the consistent observation that spontaneous low-frequency fluctuations in fMRI signal show temporal correlations between functionally related areas of the brain, even at rest (Fox & Raichle, 2007). The magnitude of these temporal correlations between different brain regions has been shown to be associated with a variety of performance measures and to be sensitive to pathology (Fox & Greicius, 2010). However, the usefulness of rsFC for assessing MLR or CLR contributions to normal locomotor control has not been previously evaluated. Therefore, the purpose of this study was to determine the association between the rsFC of subcortical locomotor regions and out-of-scanner walking performance among human adults without mobility disability. We hypothesized that rsFC of both the MLR and CLR would be significantly associated with walking capacity.

2 | MATERIALS AND METHODS

2.1 | Data source and participants

This cross-sectional study used data from the Nathan Kline Institute/Rockland Sample (NKI-RS) pilot study, available through the 1,000 Functional Connectomes Project (http://fcon_1000.projects.nitrc.org/indi/pro/nki.html) (Nooner et al., 2012). The NKI-RS pilot obtained

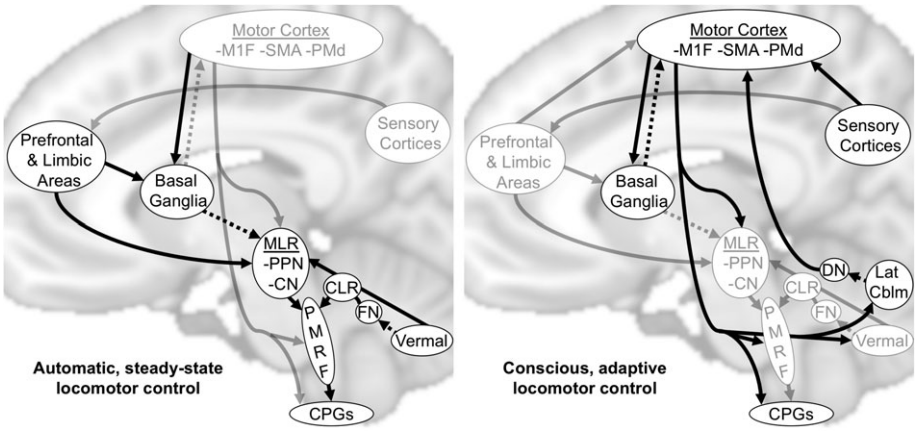

FIGURE 1 Conceptual models of locomotor control. Arrows show supraspinal connections thought to be the most relevant for automatic and conscious locomotor control, with the most emphasized connections for each type of locomotor control shown in black. Known inhibitory connectivity is shown by dashed lines. MLR, midbrain locomotor region; CLR, cerebellar locomotor region; M1F, primary motor cortex foot area; SMA, supplemental motor area; PMd, dorsal premotor cortex; PPN, pedunculopontine nuclei; CN, cuneiform nuclei; FN, fastigial nuclei; DN, dentate nuclei; Lat Cblm, lateral cerebellum; PMRF, pontomedulary reticular formation; CPGs, central pattern generators

phenotypic data, tissue, and brain imaging data from a convenience sample of 250 individuals aged 4–89 years, living in the area of Rockland County, NY, who consented to unrestricted distribution of their anonymized data (Nooner et al., 2012). To be included in the current analysis, participants had to meet all the following criteria: (1) age ≥ 18 years; (2) available data for the 6-min walk test (6MWT), age, sex, height, and body mass index (BMI); (3) an available T1-weighted MRI; (4) an available resting-state fMRI scan with <26 out of 260 (10%) motion outlier volumes; and (5) no recorded diagnoses of nervous, circulatory, respiratory, or musculoskeletal system disorders.

2.2 | Phenotypic data

The primary independent variable for this analysis was the 6MWT distance, which measures how far a participant is able to walk in 6 minutes, with instruction and standardized encouragement to walk "as far as possible" (ATS Committee on Proficiency Standards for Clinical Pulmonary Function Laboratories, 2002). Median 6MWT distance among healthy 40–80 year olds is 576 m for males and 494 m for females (Enright & Sherrill, 1998). Clinically important difference estimates range from about 20 to 50 m (Perera, Mody, Woodman, & Studenski, 2006). Across populations, possible contibutors to 6MWT performance include aerobic fitness (i.e., cardiovascular, respiratory, and metabolic capacity), anthropometric factors (e.g., height and body mass), neuromuscular factors (e.g., strength, locomotor control), and psychological factors (e.g., motivation) (ATS Committee on Proficiency Standards for Clinical Pulmonary Function Laboratories, 2002; Enright & Sherrill, 1998; Gibbons et al., 2001; Troosters, Gosselink, & Decramer, 1999).

Among healthy adults, evidence suggests that aerobic fitness and strength do not limit 6MWT performance and that locomotor control, anthropomorphic factors, and motivation are likely the primary determinants. In this population, cardiovascular responses during the 6MWT are low (e.g., median heart rate increases of 20–25 bpm; Enright & Sherrill, 1998; Troosters et al., 1999) and there is minimal decline in speed across the 6 min (e.g., 1.98 m/s pace during the first 2 min vs 1.94 m/s overall) (Gibbons et al., 2001). Age, sex, height, and body mass explain ~40% of the variability in 6MWT performance among healthy adults (Enright & Sherrill, 1998; Gibbons et al., 2001; Troosters et al., 1999), and accounting for these factors has been shown to explain the association between 6MWT distance and quadriceps strength (Troosters et al., 1999).

Additional cofactors used for this analysis included age, sex, height, BMI, resting heart rate, systolic blood pressure rating prior to the 6MWT, dyspnea rating, the Beck Depression Inventory II score, and the Wechsler abbreviated scale of intelligence block design score (Nooner et al., 2012).

2.3 | MRI data acquisition

The NKI-RS pilot study used a Siemens MAGNETOM Trio 3 T MRI system. The following scans were used in this analysis:

- T1-weighted structural images, acquired with the following MPRAGE sequence parameters: voxel size, 1.0 mm^3; TR, 2,500 ms; TE, 3.5 ms; flip angle, 8°.
- Resting-state fMRI time series, acquired with the following EPI sequence parameters: voxel size, 3.0 mm^3; TR, 2.5 s; acquisition time, 10:55 (260 volumes after discarding the first 2); TE, 30 ms; flip angle, 80°; interleaved slice sequence.

2.4 | Structural MRI data processing

Bias-corrected structural T1 images were nonlinearly transformed to the FSL MNI152 2 mm brain template using FSL FNIRT (Jenkinson, Beckmann, Behrens, Woolrich, & Smith, 2012). Separately, the native subject space T1 images were also segmented to obtain white matter and cerebrospinal fluid masks using the CONN toolbox (Whitfield-Gabrieli and Nieto-Castanon, 2012) for SPM (http://www.fil.ion.ucl.ac.uk/spm/). The subject space segmentations were then transformed to MNI space using the same nonlinear warp that was applied to the full T1 image.

2.5 | Functional MRI data processing

Resting-state functional images were initially processed using the CONN default preprocessing pipeline for volume-based analyses, including motion correction (realignment and unwarp), slice-timing correction, and outlier detection (using a 97% threshold on motion parameters) (Whitfield-Gabrieli and Nieto-Castanon, 2012). FSL was then used to register the functional scan with the native subject space T1 (FLIRT with boundary-based registration) and transform to FSL MNI152 2 mm brain space (FNIRT) in a single step. The majority of the analyses used unsmoothed functional data averaged within regions of interest (ROIs), but an 8 mm FWHM smoothed functional file was also generated for voxel-level visualizations.

The CONN denoising pipeline was implemented to regress confounding effects out of the BOLD signal, including (1) regression of 5 principle components and their temporal derivatives from both the white matter and cerebrospinal fluid time series extracted from the structural masks described above; (2) regression of the 6 head motion parameters and their temporal derivatives; and (3) scrubbing of outlier volumes. Temporal filtering (0.008–0.09 Hz) and linear detrending were also applied. For denoising, the white matter masks were reduced to minimize the chances of regressing out biologic signal of interest, especially in subcortical regions where gray and white matter tissue probabilities are intermediate. We removed any white matter mask overlap with the CONN atlas, the brainstem or within 5 mm of any regions of interest, then eroded the white matter masks by an additional 2 mm.

2.6 | fMRI head motion covariates

In addition to the fMRI realignment, unwarping, head motion parameter regression, and scrubbing described above for first-level (within-participant) preprocessing, the analyses also included two fMRI head motion summary measures for each participant as second level (between-participant) covariates. These motion summary measures

were the number of outlier volumes in the resting-state fMRI scan and average framewise displacement during the scan summed across the 6 motion parameters (Power, Barnes, Snyder, Schlaggar, & Petersen, 2012).

2.7 | Seed selection

Based on previous studies (Bohnen & Jahn, 2013; Jahn et al., 2008a; Takakusaki, 2013), our primary seed regions were the midbrain locomotor region (MLR) and cerebellar locomotor region (CLR). As the PPN is the most widely studied component of the MLR and is difficult to isolate from other MLR structures (Sebille et al., 2017), we used the PPN deep brain stimulation ROI from Fox et al. (2014) as the MLR seed (3 mm radius sphere centered at MNI coordinates ±6, −27, −15). This seed was based on stereotactic localization and voxel-based morphometry (Fox et al., 2014) and its coordinates are nearly identical to those from a study involving manual PPN tracing in Talairach space (Peterson, Pickett, Duncan, Perlmutter, & Earhart, 2014), after transformation to MNI space (±6, −26, −15) using tal2mni (http://imaging.mrc-cbu.cam.ac.uk/imaging/MniTalairach) (Brett, Johnsrude, & Owen, 2002). For the CLR, we used 6-mm-radius spheres (Fasano et al., 2017) centered at the cerebellar coordinates of a task fMRI activation focus during active versus passive stepping among healthy adults (−8, −42, −26; +8, −44, −26; Jaeger et al., 2014), masked with the FSL MNI152 template brain. These coordinates are in close proximity to white matter and the fastigial nuclei, which is consistent with how the CLR is described in the animal literature (Mori et al., 2001). As several alternative coordinates in the literature could potentially be used to represent the MLR and CLR (Cremers et al., 2012; Fasano et al., 2017; Fling et al., 2013; Fling et al., 2014; Jahn et al., 2008a; Karachi et al., 2010; Peterson et al., 2014; Snijders et al., 2011; Snijders et al., 2016), we also assessed how specific the results were to the chosen seed coordinates in a secondary analysis described below. Further details about the selection of seed coordinates are also included in Section 4.

2.8 | Target ROI selection

To identify gait-related ROIs, we performed an activation likelihood estimation (ALE) meta-analysis and used the results to select ROIs from a whole-brain parcellation. To be included in the meta-analysis, brain foci coordinates had to meet the following criteria: (1) positive activation foci from contrasting actual or imagined locomotion with a nongait task (e.g., rest, imagined lying) among healthy adults; (2) coordinates reported to be in MNI or Talairach space (Talairach coordinates were converted to MNI using tal2icbm_fsl; http://www.brainmap.org/icbm2tal; Lancaster et al., 2007). Included studies are listed in Section 3. Task contrasts were excluded if they were redundant with a previous contrast from the same study (i.e., same participants and locomotor task with a different nongait comparison). Random-effects, nonadditive ALE meta-analysis was performed with GingerALE v2.3 (Turkeltaub et al., 2012), using a voxel-wise significance threshold of $p < .01$ (uncorrected).

We created a whole-brain parcellation by starting with the 246 parcels of the Brainnetome atlas (http://atlas.brainnetome.org/download.html, BN_Atlas_246_2mm.nii.gz) (Fan et al., 2016), and adding the 50 cerebellar and brainstem parcels from Shen et al. (https://www.nitrc.org/frs/?group_id=51,shen_2mm_268_parcellation.nii.gz) (Finn et al., 2015; Shen, Tokoglu, Papademetris, & Constable, 2013). This combined 296 parcel Brainnetome-Shen (BnS) atlas in MNI152 2 mm template space and parcel information (e.g., Brainnetome cytoarchitectural labels) are available as supplemental files. BnS parcels that had at least 15 voxels of overlap with the significance map from gait-related ALE meta-analysis were included as target ROIs for the subsequent analyses.

2.9 | Primary analysis

Functional connectivity analysis was performed using MATLAB and FSL's Permutation Analysis of Linear Models (PALM) (Winkler, Ridgway, Webster, Smith, & Nichols, 2014). For each participant, Fisher z transformed temporal correlations were calculated from each seed (MLR and CLR) to each of the gait-related target ROIs. The association between these Fisher *z* connectivity values and 6MWT distance was then tested for all target ROIs to identify regions where individual differences in rsFC were associated with differences in walking capacity. Analyses were adjusted for age, sex, height, BMI, and the two summary fMRI head motion measures by adding nuisance regressors to the second level (between-participant) model. Nonparametric statistics were calculated using 5,000 permutations. The primary analysis was thresholded at a false discovery rate (FDR) corrected $p < .05$.

2.10 | Seed rsFC descriptive statistics

To assist with comparison to previous studies (Fasano et al., 2017; Fox et al., 2014), we created seed-to-voxel rsFC maps to visualize the topography of each seed's mean connectivity. To aid in the interpretation of significant seed-to-ROI rsFC–6MWT associations, we also calculated descriptive statistics for the underlying seed-to-ROI rsFC. For example, if a positive rsFC–6MWT association target ROI was in an area of entirely positive (rather than negative) rsFC, it would indicate that more positive (rather than less negative) rsFC is associated with greater walking capacity. Likewise, if a negative rsFC–6MWT association target ROI was in an area of no significant rsFC, it could indicate that positive rsFC is atypical and is associated with poorer walking capacity, and/or that negative rsFC is atypical and is associated with greater walking capacity.

2.11 | Bivariate rsFC associations with phenotypic variables

To further facilitate the interpretation of significant seed-to-ROI rsFC–6MWT associations, we computed bivariate associations between the seed-to-ROI rsFC values and each of the phenotypic variables.

2.12 | Testing the independence of multiple rsFC–6MWT associations

We also sought to evaluate whether each identified seed-to-ROI pair provided information about walking capacity that was independent from the other seed-to-ROI pairs and independent from other

covariates. To this end, we performed a multiple linear regression analysis with 6MWT distance as the dependent variable, each locomotion-related seed-to-ROI pair as an independent variable of interest and the other nonlocomotor phenotypic variables as covariates. Seed-to-ROI pairs providing independent information related to walking capacity would still remain statistically significant after adjusting for all other variables in the model.

2.13 | Normative data visualizations for cortical ROIs showing gait-related rsFC

In addition, we aimed to assess the probability of structural connectivity between seeds and ROIs with gait-related rsFC. For Brainnetome Atlas ROIs that were part of significant rsFC–6MWT associations, we used available probabilistic tractography maps (http://atlas.brainnetome.org/download.html, BNA_SC_4D.nii.gz) to visualize ROI structural connectivity in the regions of the MLR and CLR. Fan et al. (2016) created these maps using diffusion MRI data from 40 healthy adults (age 22–35). They performed probabilistic tractography from each voxel in the ROI to every other brain voxel with 5,000 samples, thresholded at 25% probability and a raw trace count ≥2, then binarized and combined the tractograms across participants to create the group probability maps, which they thresholded at 25% and made publicly available (Fan et al., 2016).

Further, we sought to assess functional brain network membership for ROIs with gait-related rsFC. For Brainnetome Atlas ROIs that were part of significant rsFC–6MWT associations, we used available probabilistic rsFC maps (BNA_FC_4D.nii.gz) to visualize normative ROI rsFC in relation to known functional networks. Fan et al. (2016) created these maps using resting-state fMRI data from 40 healthy adults. They Fisher *z* transformed individual ROI-to-voxel rsFC maps, thresholded at $p_{FDR} < .05$ with a minimum cluster extent of 50 voxels, then binarized and combined maps across participants. Fan et al. (2016) then thresholded these group probability maps at 25% and made them publicly available. For this visualization, we displayed these probabilistic rsFC outlines as an overlay above cortical network labels (http://surfer.nmr.mgh.harvard.edu/fswiki/CorticalParcellation_Yeo2011) (Yeo et al., 2011).

2.14 | Control seeds

To evaluate how specific the results were to the MLR and CLR, we also included several control seeds in the motor cortex. These control seeds were in the primary motor cortex foot area (M1F), supplemental motor area (SMA), and dorsal premotor cortex (PMd), using 6-mm-radius spheres centered on the coordinates used by previous studies (M1F ±6, −26, +76; SMA ±31, −5, 68; PMd 0, 1, 63) (Buckner et al., 2011; Fox et al., 2014). For each of these control seeds, we first repeated the primary analysis for comparison with the MLR and CLR seed results.

However, this method of comparison could be sensitive to the chosen statistical thresholds. Therefore, we also calculated two summary effect size measures of the overall association between each seed and walking capacity. These seed summary measures were the mean and maximum rsFC–6MWT T score absolute values across all target ROIs. Higher mean and maximum T scores for a particular seed indicate that its rsFC has a greater overall association with walking capacity, regardless of the anatomical location of the seed's gait-related rsFC (within the 81 target ROIs). We also statistically compared the seed-to-ROI T scores of the control seeds with the corresponding T scores from the a priori MLR and CLR seeds, using nonparametric Wilcoxon signed-rank tests with FDR correction.

2.15 | MLR and CLR seed specificity analyses

To evaluate how specific the MLR and CLR results were to the chosen seed coordinates, we first repeated the primary analysis for several alternative MLR and CLR seed locations from the literature. Similar to the control seeds, we additionally calculated summary rsFC–6MWT effect size measures for each of the alternative MLR and CLR seeds and statistically compared them with the a priori seeds.

3 | RESULTS

From 207 participants with available data in the NKI-RS pilot study, participants were excluded from this analysis for missing 6MWT data (*n* = 39), age < 18 years (*n* = 39), missing height and weight (*n* = 1), missing T1 MRI (*n* = 1), and having ≥26 out of 260 (10%) motion outlier volumes in the resting-state fMRI scan (*n* = 8); leaving 119 eligible participants aged 18–85 years with complete data for this analysis. Participant characteristics and fMRI head motion summary measures are shown in Table 1.

3.1 | Meta-analysis results and ROI selection

Twenty-one task contrasts involving 433 total participants from 17 studies met eligibility criteria for the meta-analysis and reported 333 gait-related activation foci (Allali et al., 2014; Bakker et al., 2008; Cremers et al., 2012; la Fougere et al., 2010; Godde and Voelcker-Rehage, 2010; Iseki, Hanakawa, Shinozaki, Nankaku, & Fukuyama,

TABLE 1 Participant characteristics (*n* = 119)

Phenotypic variables	
Six-minute walk test distance, *m*	333 ± 76
Age, years	41 ± 19
Males, *n* (%)	71 (60%)
Height, inch	67 ± 6
Body mass index, kg/m^2	27 ± 5
Resting heart rate, bpm	72 ± 10
Resting systolic blood pressure, mmHg	118 ± 12
Dyspnea rating >0, *n* (%)	14 (12%)
Beck depression inventory II score, 0–63	5 ± 7
Visual constructional ability (WASI block design T score), 20–80	55 ± 8
fMRI head motion summary measures	
Number of outlier volumes, 0–260	4 ± 5
Average frame-wise displacement[a], mm	0.13 ±0.08

WASI = Wechsler abbreviated scale of intelligence. Data presented as mean ± *SD* or *n* (%).

[a] Frame-by-frame movement summed across 6 motion parameters and averaged across scan.

2008; Hanakawa et al., 1999; Jaeger et al., 2014; Jaeger et al., 2016; Jahn et al., 2008b; Jahn et al., 2004; Karachi et al., 2012; Martinez et al., 2016; van der Meulen, Allali, Rieger, Assal, & Vuilleumier, 2014; Wagner et al., 2008; Wutte, Glasauer, Jahn, & Flanagin, 2012; Zwergal et al., 2012). The ALE significance map ($p < .01$, uncorrected) included 6,790 voxels (54,320 mm^3) distributed across the brain with the largest clusters in the anterior, superior, medial cerebellum, medial motor cortices, and bilateral anterior insular cortices (Supporting Information, Figure S1). Eighty-one out of 296 parcels (27%) from the BnS atlas had ≥15 voxels (120 mm^3) with gait-related ALE $p < .01$. These 81 parcels were included as ROIs in the subsequent analyses.

3.2 | Primary analysis results and rsFC descriptive statistics

In the primary analysis, MLR rsFC with an ROI in the right superior frontal gyrus (SFG) adjacent to the anterior cingulate cortex (ACC) was positively associated with 6MWT distance (Figure 2 and Table 2). This ROI was largely within an area of positive MLR rsFC. MLR rsFC with an ROI in the right paravermal cerebellum was also positively associated with 6MWT distance. This ROI was entirely within an area of positive MLR rsFC. CLR rsFC with an ROI in the left anterior paracentral lobule (M1F) was negatively associated with the 6MWT. Although this ROI as a whole showed positive CLR rsFC (Table 2), it was predominantly in an area of no CLR rsFC (Figure 2).

3.3 | Bivariate rsFC associations with phenotypic variables

Post-hoc analyses focused on the three seed-to-ROI rsFC pairs that were significantly associated with the 6MWT in the primary analysis. Bivariate correlations between these seed-to-ROI rsFC values and other participant data are presented in Table 3. MLR–SFG/ACC rsFC was negatively correlated with resting heart rate and blood pressure.

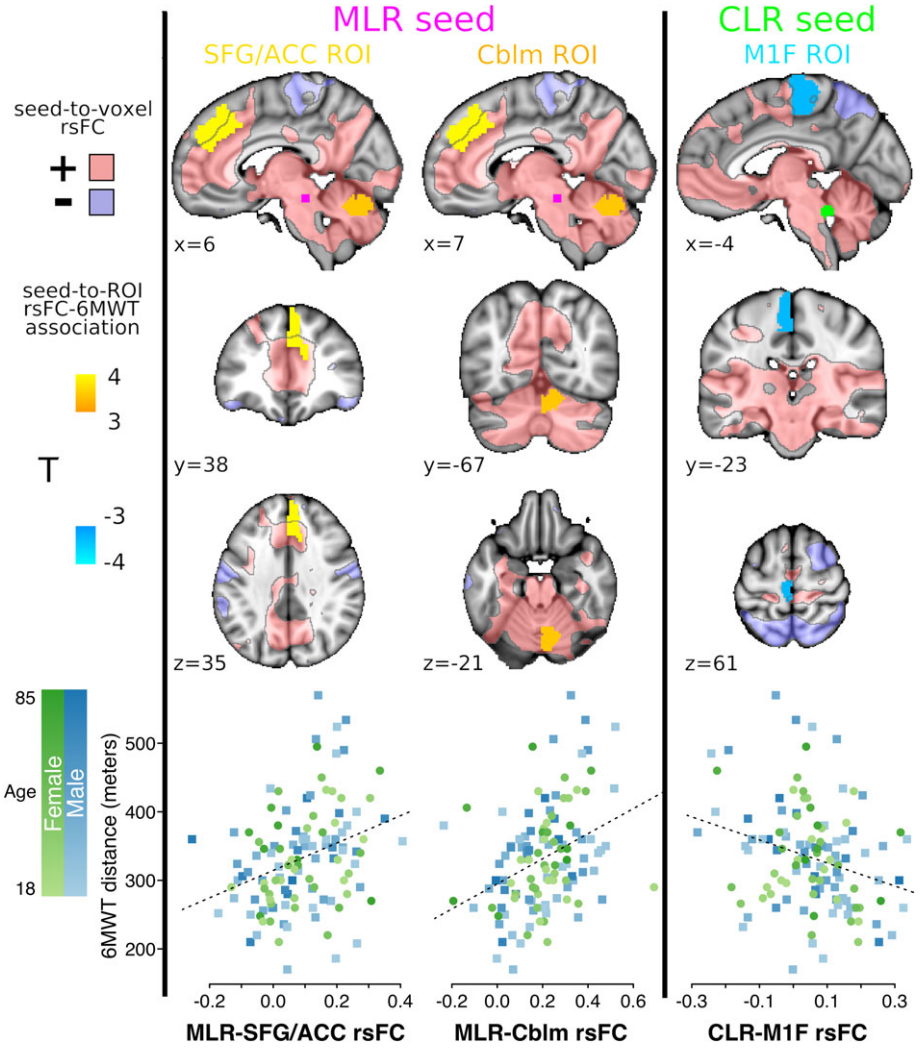

FIGURE 2 Primary MLR and CLR rsFC associations with walking capacity ($n = 119$). Seed-to-ROI rsFC significantly associated with 6MWT distance (two-sided nonparametric $p_{FDR} < 0.05$), shown in MNI152 space at ROI centroid coordinates. Areas with positive and negative mean seed-to-voxel rsFC ($|T| > 2$) are translucently shown in pink and purple, respectively, with black outlines. The bottom row shows Fisher *z* rsFC values for each gait-related rsFC pair plotted against 6MWT distance, with color coding for participant age and sex. MLR, midbrain locomotor region; CLR, cerebellar locomotor region; rsFC, resting-state functional connectivity; 6MWT, 6-min walk test; SFG, superior frontal gyrus; ACC, anterior cingulate cortex; Cblm, cerebellum; M1F, primary motor cortex foot area; FDR, false discovery rate

TABLE 2 MLR and CLR seed-to-ROI rsFC significantly associated with 6MWT distance (n = 119)

Seed	ROI BnS #, orig #, label	ROI centroid MNI coordinates (mm)	Mean ± *SD* [95% CI] rsFC (Fisher z)	6MWT association T	p_{FDR}	$p_{uncorrected}$
MLR	12, Bn12, right superior frontal gyrus medial area 9	6, 38, 35	0.09 ± 0.12 [0.07, 0.11]	3.96	.0162	.0002
MLR	253, S106, right paravermal cerebellum	7, −67, −21	0.21 ± 0.15 [0.18, 0.23]	3.57	.0162	.0004
CLR	67, Bn67, left paracentral lobule area 4 (M1F)	−4, −23, 61	0.06 ± 0.13 [0.03, 0.08]	−3.46	.0486	.0006

MLR = midbrain locomotor region; CLR = cerebellar locomotor region; ROI = region of interest; rsFC = resting-state functional connectivity; 6MWT = 6-min walk test; Bn = Brainnetome Atlas; S = Shen Atlas; MNI = Montreal Neurological Institute space; CI = confidence interval; M1F = primary motor cortex foot area. 6MWT-rsFC association testing was nonparametric, two-sided, adjusted for age, sex, height, and body mass index, and false-discovery rate (FDR) corrected for 81 ROI comparisons with a significance threshold of $p_{FDR} < .05$.

MLR–cerebellum connectivity was positively correlated with the number of fMRI motion outlier volumes and negatively correlated with depression score and visuoconstructional ability. CLR–M1F connectivity was positively correlated with depression score and negatively correlated with the other two rsFC values.

3.4 | Independence of the three rsFC–6MWT associations

In multiple linear regression analysis with 6MWT distance as the dependent variable, the two MLR rsFC variables remained statistically significant after adjusting for all other variables (Table 4). Thus, each MLR rsFC variable showed an independent association with walking function, including independence from both the other rsFC variables and the phenotypic variables. The MLR rsFC variables also exhibited stronger 6MWT partial correlations than all other variables, indicating a greater association with walking capacity. Furthermore, phenotypic associations with the 6MWT decreased and none were significant with the rsFC variables in the model, indicating that the rsFC variables explained some of the association between the phenotypic variables and walking capacity.

When including only the three rsFC variables in the model, R^2 was 0.25, indicating that 25% of the total variance in walking capacity could be explained based on these rsFC values alone. Regression coefficients for the MLR rsFC variables were 185 (MLR–SFG/ACC connectivity) and 164 (MLR–cerebellum connectivity), indicating that Fisher z connectivity differences of +0.2 were associated with clinically meaningful 6MWT differences of approximately +37 and +33 m, respectively. The CLR–M1F rsFC association with the 6MWT remained significant when adjusting for MLR–SFG/ACC rsFC only, but decreased and became nonsignificant when adjusting for MLR–cerebellum rsFC. Thus, some of the 6MWT variance associated with CLR–M1F rsFC could be explained by MLR–cerebellum rsFC.

3.5 | Normative structural and functional connectivity of cortical ROIs with gait-related rsFC

As two of the significant gait-related rsFC pairs from the primary analysis involved cortical ROIs from the Brainnetome atlas (right SFG/ACC and left M1F ROIs; BnS 12 and 67), we were able to visualize probabilistic tractography and probabilistic rsFC maps for these regions using the results from Fan et al. (2016). Each of these ROIs showed structural connectivity with both the MLR and CLR bilaterally (Supporting Information,

TABLE 3 Correlations between walking capacity, rsFC values, and covariates (n = 119)

	6MWT	MLR–SFG/ACC connectivity	MLR–cerebelulm connectivity	CLR–M1F connectivity
6MWT distance	1	0.33 (<0.001)	0.37 (<0.001)	−0.28 (0.002)
rsFC: MLR–SFG/ACC (BnS 12)	0.33 (<0.001)	1	0.01 (0.944)	−0.20 (0.027)
rsFC: MLR–cerebellum (BnS 253)	0.37 (<0.001)	0.01 (0.944)	1	−0.34 (<0.001)
rsFC: CLR–M1F (BnS 67)	−0.28 (0.002)	−0.20 (0.027)	−0.34 (<0.001)	1
No. fMRI motion outlier volumes	0.16 (0.078)	−0.05 (0.611)	0.28 (0.002)	0.07 (0.473)
Mean fMRI framewise displacement	0.01 (0.953)	0.07 (0.445)	0.13 (0.166)	0.09 (0.315)
Age	−0.13 (0.144)	0.02 (0.795)	−0.14 (0.119)	0.00 (0.979)
Male sex	0.01 (0.905)	−0.03 (0.735)	−0.03 (0.787)	0.02 (0.813)
Height	0.12 (0.177)	0.05 (0.587)	0.04 (0.659)	0.07 (0.470)
Body mass index	−0.05 (0.600)	0.01 (0.939)	0.05 (0.627)	−0.16 (0.082)
Resting heart rate	−0.27 (0.003)	−0.20 (0.026)	−0.11 (0.235)	0.12 (0.205)
Resting systolic blood pressure	−0.22 (0.018)	−0.09 (0.325)	−0.10 (0.256)	0.09 (0.313)
Dyspnea rating	−0.09 (0.334)	0.04 (0.669)	−0.03 (0.741)	−0.05 (0.580)
Depression score (BDI)	−0.16 (0.088)	−0.03 (0.716)	−0.19 (0.038)	0.28 (0.002)
Visuoconstructional ability (WASI-BD)	−0.06 (0.491)	−0.08 (0.386)	−0.24 (0.009)	0.10 (0.266)

rsFC = resting-state functional connectivity; 6MWT = 6-min walk test; MLR = midbrain locomotor region; SFG = superior frontal gyrus; ACC = anterior cingulate cortex; CLR = cerebellar locomotor region; M1F = primary motor cortex foot area; BDI = Beck Depression Inventory II; WASI-BD = Wechsler abbreviated scale of intelligence - block design.
Values are Pearson r (p value).

TABLE 4 Results of 6MWT multiple linear regression analysis (n = 119)

Model with all covariates					
	Estimate	**Std. error**	***t* value**	**Pr(>|*t*|)**	**Partial correlation**
(Intercept)	282.08	112.65	2.50	0.0138	0.00
rsFC: MLR–SFG/ACC (BnS 12), Fisher *z*	174.52	52.87	3.30	0.0013	0.29
rsFC: MLR–cerebellum (BnS 253), Fisher *z*	126.90	48.13	2.64	0.0097	0.25
rsFC: CLR–M1F (BnS 67), Fisher *z*	−70.32	57.95	−1.21	0.2277	−0.12
No. fMRI motion outlier volumes, 0–260	2.85	1.48	1.93	0.0566	0.20
Mean fMRI framewise displacement, mm	−116.91	110.84	−1.06	0.2940	−0.12
Age, years	0.04	0.44	0.09	0.9276	0.01
Male sex	−2.82	14.43	−0.20	0.8457	−0.02
Height, inch	1.93	1.30	1.48	0.1410	0.14
Body mass index, kg/m^2	0.85	1.56	0.55	0.5870	0.06
Resting heart rate, bpm	−0.78	0.91	−0.86	0.3921	−0.10
Resting systolic blood pressure, mmHg	−0.73	0.79	−0.93	0.3568	−0.11
Dyspnea rating, 0–4	−18.82	15.57	−1.21	0.2294	−0.10
Depression score (BDI), 0–63	−0.38	1.73	−0.22	0.8243	−0.02
Visuoconstructional ability (WASI-BD), 20–80	0.22	0.86	0.25	0.8035	0.02
Residual standard error: 66.04 on 104 degrees of freedom. Multiple R-squared: 0.3261, adjusted R-squared: 0.2354. F-statistic: 3.595 on 14 and 104 DF, *p* value: 7.65e-05.					
Model with rsFC variables only					
	Estimate	**Std. error**	***t* value**	**Pr(>|*t*|)**	**Partial correlation**
(Intercept)	285.71	13.21	21.63	0.0000	0.00
rsFC: MLR–SFG/ACC (BnS 12), Fisher *z*	185.21	50.39	3.68	0.0004	0.30
rsFC: MLR–cerebellum (BnS 253), Fisher *z*	164.01	42.92	3.82	0.0002	0.33
rsFC: CLR–M1F (BnS 67), Fisher *z*	−64.10	52.87	−1.21	0.2279	−0.11
Residual standard error: 66.26 on 115 degrees of freedom. Multiple R-squared: 0.2497, adjusted R-squared: 0.2302. F-statistic: 12.76 on 3 and 115 DF, *p* value: 2.949e-07.					

6MWT = 6-minute walk test; rsFC = resting-state functional connectivity; MLR = midbrain locomotor region; CLR = cerebellar locomotor region; SFG = superior frontal gyrus, ACC = anterior cingulate cortex; M1F = primary motor cortex foot/leg area; BDI = Beck depression inventory II; WASI-BD = Wechsler abbreviated scale of intelligence - block design.

Figure S2). The right SFG/ACC ROI showed positive probabilistic rsFC across most of the default mode and frontoparietal network regions and negative rsFC across most of the cortical somatomotor, dorsal attential, and visual network regions (Supporting Information, Figure S3). The left M1F ROI showed positive rsFC across most of the somotomotor network and some of the visual network regions and negative rsFC across most of the frontoparietal network regions.

3.6 | Control seed results

When repeating the primary analysis with the cortical control seeds (M1F, SMA, and PMd), no significant rsFC–6MWT associations were found. The a priori MLR and CLR seeds had significantly higher mean rsFC–6MWT association magnitudes (averaged across the target ROIs) than the SMA seed, but not the M1F or PMd seeds (Table 5).

3.7 | Specificity of the rsFC–6MWT results to the selected seeds

Given that there is no consensus on the correct coordinates for the MLR or CLR, we also explored whether substituting our a priori seeds with 8 alternative MLR seeds and 6 alternative CLR seeds would result in stronger associations with walking capacity (Table 5). Of these alternative coordinates, only the Peterson et al. (2014) MLR seeds showed a significant rsFC–6MWT association at the FDR-corrected threshold used for the primary analysis. These Peterson MLR seeds were nearly identical to our a priori MLR seed from Fox et al. (2014) and resulted in similar rsFC–6MWT association ROIs compared with our primary analysis (Table 5). Our a priori MLR seed showed a significantly higher mean rsFC–6MWT association magnitude than each of the alternative MLR seeds, except those from Peterson et al. (2014) and Fling et al. (2014). Our a priori CLR seed showed a significantly higher mean rsFC–6MWT association magnitude than every alternative CLR seed.

4 | DISCUSSION

This study tested the association between brain locomotor region rsFC and walking capacity among human adults without mobility disability. Similar to previous studies (Fox et al., 2014; Fasano et al., 2017), the MLR showed negative rsFC with the medial motor cortex and positive rsFC across many diverse brain regions, while the CLR showed positive (albeit weak) rsFC with the motor cortex (among many diverse regions) and negative or no rsFC with areas of the premotor, prefrontal, and parietal cortices (Figure 2). Significant rsFC associations with walking

TABLE 5 ROI location specificity analysis (n = 119). Mean seed rsFC association with walking capacity across ROIs for the a priori, alternative, and control seeds

Seed	Reference	Seed coordinates	Mean |T|	Max |T|	Significant rsFC–6MWT association ROIs (p_{FDR} < .05)
MLR	Peterson 2014*	±6, −26, −15	1.23	3.67	12
	Peterson 2014†	−5/+8, −27, −14	1.19	3.56	253
	Fox 2014	±6, −27, −15	1.16	3.96	12, 253
	Fling 2013	±7, −32, −22	0.94	2.77	None
	Cremers 2012	±4, −26, −22	0.85[m]	2.88	None
	Karachi 2010	±3, −22, −13	0.79[m]	2.52	None
	Snijders 2011	0, −28, −20	0.77[m]	2.32	None
	Snijders 2016	±6, −33, −20	0.71[m]	2.49	None
	Fling 2014	−5/+8, −32, −22	0.70[m]	2.17	None
CLR	*Jaeger 2014*	±8, −42/−44, −26	1.15	3.46	(67)
	Peterson 2014†	0/+2, −49, −28	0.91[c]	2.65	None
	Jahn 2008*	±6, −48, −14	0.89[c]	3.21	None
	Peterson 2014*	0, −46, −33	0.87[c]	2.08	None
	Cremers 2012	±2, −58, −16	0.77[c]	3.06	None
	Fling 2014	−6/+9, −55, −18	0.73[c]	3.10	None
	Fasano 2017	−20/+16, −44, −26	0.68[c]	2.35	None
M1F	Buckner 2011	±6, −26, 76	1.01	3.45	None
SMA	Fox 2014	0, 1, 63	0.69[mc]	2.23	None
PMd	Fox 2014	±31, −5, 68	1.03	2.77	None

rsFC = resting-state functional connectivity; ROI = region of interest; MLR = midbrain locomotor region; CLR = cerebellar locomotor region; M1F = primary motor cortex foot area; SMA = supplemental motor area; PMd = dorsal premotor cortex. 6MWT = 6-min walk test; FDR = false discovery rate corrected. Seeds were spheres centered on given coordinates with 3 mm radius for MLR and 6 mm radius for CLR, M1F, SMA, and PMd. Italicized seeds were a priori primary seeds. For each seed, the absolute values of the rsFC–6MWT association T values (adjusted for age, sex, height, body mass index, and summary head motion measures) were obtained for all 81 ROIs to calculate mean and max |T|. Alternative seeds are ordered by this mean |T| value. In the far-right column, the ROI number in parentheses denotes a negative rsFC–6MWT association.
*Brett transformed from Talairach to MNI152 space using tal2mni (http://imaging.mrc-cbu.cam.ac.uk/imaging/MniTalairach) [Brett et al., 2002].
†Lancaster transformed from Talairach to FSL MNI152 space using tal2icbm_fsl (http://www.brainmap.org/icbm2tal) [Lancaster et al., 2007].

capacity were found with adjustment for age, sex, height, BMI, and fMRI head motion at conservative statistical thresholds (two-sided nonparametric p_{FDR} <.05, adjusted for 81 seed-to-ROI tests). Specifically, greater MLR connectivity with the superior frontal gyrus (SFG) adjacent to the anterior cingulate cortex (ACC) and greater MLR connectivity with the paravermal cerebellum were each associated with greater 6MWT distance, while greater CLR connectivity with the primary motor cortex foot area (M1F) was associated with lesser 6MWT distance. Both of the MLR functional connections were independently associated with walking capacity and each explained more of the variability in 6MWT distance than any other variable (e.g., age, sex, height, and BMI). These findings suggest that functional MRI rsFC can provide important biomarkers of brain locomotor physiology.

4.1 | Interpretation of significant MLR rsFC–6MWT associations

These findings are also largely consistent with current understanding of locomotor control. For example, the positive association between MLR–cerebellum connectivity and walking capacity observed in this study is consistent with the importance of automatic, rhythmic, excitatory input to the MLR from the vermis and paravermal cerebellum, as has been previously shown in cats (Armstrong, 1988).

Likewise, the observed walking capacity association with MLR–SFG/ACC connectivity is also consistent with previous research. Although the SFG/ACC region has not traditionally been considered to be a key locomotor area, converging evidence suggests that it may be more relevant than previously appreciated. This region has shown activation during imagined walking in five previous studies among healthy adults (Allali et al., 2014; Cremers et al., 2012; la Fougere et al., 2010; Jahn et al., 2008b; van der Meulen et al., 2014), as seen in our meta-analysis (Supporting Information, Figure S1). The magnitude of this activation was also shown to be decreased in Parkinson's Disease(Snijders et al., 2011) and increased among patients with better gait function (Cremers et al., 2012). In addition, decreased ACC integrity has been associated with increased gait variability among older adults (Tian et al., 2017). Furthermore, electroencephalographic recording over the SFG/ACC region during treadmill gait in healthy

young adults has shown that this region is rhythmically active in synchrony with the gait cycle (Gwin et al., 2011; Knaepen et al., 2015). This activity is the most pronounced during trailing limb push off and leading limb initial contact, similar to the gait-related activation pattern of the sensorimotor cortex (Gwin et al., 2011; Knaepen et al., 2015).

The ACC is preferentially activated during self-paced (vs externally paced) movement (Jenkins, Jahanshahi, Jueptner, Passingham, & Brooks, 2000), and is thought to support motivation for extended, effortful behaviors (Holroyd & Umemoto, 2016) like the 6MWT. Therefore, the positive association observed in this study between MLR–SFG/ACC connectivity and walking capacity may reflect the importance of prefrontal/limbic input to the MLR for motivational aspects of the 6MWT. If this interpretation is accurate, MLR–SFG/ACC connectivity could serve as a potential biomarker of motivation for physical activity. Although only correlative, the negative MLR–SFG/ACC rsFC association with resting heart rate and systolic blood pressure could be consistent with this interpretation, as regular endurance exercise lowers resting heart rate and systolic blood pressure (Wilmore et al., 2001). Alternatively or additionally, the SFG/ACC region may play a role in online movement error detection and correction during locomotion (Gwin et al., 2011).

4.2 | Interpretation of significant CLR rsFC–6MWT associations

Our observed negative walking capacity association with CLR–M1F connectivity is also consistent with previous studies. While the cerebral motor cortices do not appear to receive strong input from the CLR or fastigial nuclei (Allen & Tsukahara, 1974), it was more recently discovered that the medial motor and premotor areas of the cerebral cortex (including M1F) have dense outputs to the cerebellar vermis (which provides the major input to the fastigial nuclei and CLR) via the cortico-ponto-cerebellar pathway (Coffman et al., 2011). Thus, it is possible that CLR–M1F connectivity could at least partially reflect M1F input to the CLR through the pontine nuclei and vermis.

The inverse nature of the observed CLR–M1F association with walking capacity can be partly explained by the current conceptual model of Parkinsonian gait pathology. The model indicates that subcortical locomotor dysfunction causes both *decreased* walking capacity and a compensatory *increase* in conscious cortical input to the subcortical locomotor network (Peterson & Horak, 2016). This compensation is thought to be the mechanism of increased gait variability and decreased automaticity in Parkinson's Disease (Peterson & Horak, 2016). Our gait association findings suggest that greater CLR–M1F connectivity could represent this compensatory increase in conscious locomotor control.

The compensatory nature of this connectivity increase is supported by the low mean CLR–M1F correlation coefficient (Fisher *z*: 0.06 [95%CI: 0.03, 0.08]), which indicates that normal connectivity between M1F and the Jaeger et al. (2014) CLR ROI may be weak. Further, the CLR–M1F rsFC–6MWT association became nonsignificant after accounting for MLR–cerebellum rsFC, which is consistent with the hypothesis that CLR–M1F upregulation may be a compensation for downregulation of subcortical connectivity. However, it is unclear why such a compensation might be observed in the current study, which only included persons without mobility disability. It is possible that our findings reflect CLR–M1F compensation related to subclinical pathology.

However, we believe that greater CLR–M1F rsFC (and lower MLR–cerebellum rsFC) may simply be the hallmark of a more consciously controlled (rather than automatic) gait, whether as a compensation for pathology or as a maladaptive variant of normal motor behavior. This hypothesis is partly supported by a study of young healthy adults that performed near infrared spectroscopy over the motor cortex and concurrently measured gait parameters while paricipants walked on a treadmill (Kurz, Wilson, & Arpin, 2012). The authors reported that increases in M1F oxygenated hemoglobin response were temporally associated with increases in stride time variability (decreases in consistency), explaining 67% of the variance. Although speculative, our data further suggest that CLR–M1F rsFC could reflect the overall balance between conscious and automatic locomotor control. Many participants had negative CLR–M1F rsFC and greater anticorrelation appeared to positively associated with 6MWT distance (Figure 2; bottom right panel). Thus, greater walking capacity seemed to be associated with both lower CLR–M1F correlation (potentially reflecting less conscious control) and greater CLR–M1F anticorrelation (potentially reflecting more automatic control and downregulation of M1F).

Compared with the Jaeger et al. (2014) CLR location, several alternative CLR locations do appear to have stronger positive rsFC with M1F, as shown by previous research (Fasano et al., 2017) and confirmed in the current dataset. Thus, it is possible that this seed location is not the "true" CLR and that lower walking capacity in healthy adults is actually associated with cerebellar rsFC outside the normal areas of M1F connectivity, rather than increased CLR–M1F rsFC. However, the anatomical location of the Jaeger et al. (2014) seed in an area consistent with the animal CLR argues against this possibility. Furthermore, our ROI location specificity analysis showed a significantly higher mean rsFC–6MWT association for the Jaeger et al. (2014) CLR compared with every alternative CLR location tested (Table 5).

4.3 | Motor cortex rsFC and walking capacity

Two of the motor cortex control seeds (M1F and PMd) showed mean rsFC–6MWT associations of similar magnitude to our a priori MLR and CLR seeds (Table 5). However, none of the cortical seed-to-ROI connections showed a significant association with walking capacity after FDR correction for multiple comparisons. Without FDR correction, M1F and PMd showed a pattern of negative rsFC–6MWT associations with the midbrain and cerebellum and positive rsFC–6MWT associations with other motor cortex ROIs. Similar to this (nonsignificant) positive association trend, a previous study using spatial independent components analysis found that faster walking speed (20-ft walk test) was associated with greater rsFC within the cortical motor network among 30 older adults (Yuan, Blumen, Verghese, & Holtzer, 2015). Thus, basic locomotor function appears to be correlated with greater rsFC within a prefrontal-subcortical locomotor network, greater rsFC within the cortical motor network, and lesser rsFC

between these two networks. Taken together, these findings suggest that there may be some antagonism between these two networks for locomotor control.

This interpretation is also consistent with the normative structural and functional connectivity data for the two cortical ROIs that had significant rsFC–6MWT associations in our primary analysis. The right SFG/ACC ROI that was found to have gait-related rsFC with the MLR (BnS 12) has previously shown functional correlation with the default mode and frontoparietal networks and functional anticorrelation with the cortical somatomotor, dorsal attention and visual networks (Supporting Information, Figure S3) (Fan et al., 2016). Almost conversely, the left M1F ROI that was found to have a negative rsFC–6MWT association with the CLR (BnS 67) has previously shown functional correlation with the cortical somatomotor and visual networks and functional anticorrelation with the fontoparietal network (Fan et al., 2016). Yet, both these ROIs show similar structural connectivity with the CLR and MLR (Supporting Information, Figure S2). Thus, it appears that the SFG/ACC and M1F may be part of two oppositional or reciprocal brain networks with differing levels of control over different modes of locomotion (e.g., as depicted in Figure 1) or different elements of gait.

4.4 | Limitations and future study

The primary limitations to this study were that the cross-sectional observational design precluded testing causal hypotheses and that fMRI has insufficient temporal resolution to assess connectivity directionality (i.e., afferent, efferent, or reciprocal). Therefore, we had to infer potential directionality and causal relationships based on previous studies in the discussion above and alternative explanations of our findings are possible. Another limitation to our multivariate analysis is that variable noise in different brain regions could explain the independence of the 6MWT associations for the two MLR rsFC values. We do not believe this is the case based on our aggressive denoising approach and the fact that this analysis was able to identify nonindependence of the CLR–M1F rsFC value. However, we cannot completely rule out this possibility.

We were also limited to the available data and acknowledge that the 6MWT may be an imperfect measure of neural locomotor function. As age, sex, height, and BMI have been shown to influence 6MWT distance (Enright & Sherrill, 1998; Gibbons et al., 2001; Troosters et al., 1999), we adjusted for these covariates in the analysis to more specifically test rsFC associations with neural aspects of walking (e.g., locomotor control, motivation). However, residual confounding of these associations by extraneous variables is still possible and future studies with additional gait measures are needed to confirm and expand on our findings.

It is also possible that our meta-analysis and parcel selection methods may have excluded some gait-related ROIs or included some ROIs solely related to mental imagery. The majority of studies that met eligibility criteria for the meta-analysis identified gait-related activation foci using gait imagery tasks, which elicit similar but not identical brain activations compared with actual gait (la Fougere et al., 2010). Future meta-analyses aiming to identify gait-related ROIs might consider only including studies of gait-related motor performance (e.g., supine stepping) if a sufficient number of studies accumulate. However, such tasks also differ from actual walking in ways that could potentially affect brain activation (e.g., different gravity-related task demands and sensory inputs).

Another important limitation was that coordinates for the MLR and CLR are highly variable in the literature. Given this variance in ROI locations, it is not surprising (and is actually somewhat reassuring) that our results were fairly specific to our a priori MLR and CLR seed coordinates (Fox et al., 2014; Jaeger et al., 2014) and the nearly identical MLR seed coordinates from Peterson et al. (2014) (Table 5). As described in the methods, we selected our a priori coordinates based on the methodology of the reporting study, the consistency of the coordinates with known anatomic relationships, and whether coordinates were obtained in MNI space. Our results appear to confirm the validity of the a priori coordinates.

5 | CONCLUSION

Functional MRI rsFC analysis is a promising method for evaluating supraspinal mechanisms underlying variance in locomotor function. Among adults without mobility disability, greater walking capacity appears to be related to greater connectivity of the MLR with the SFG/ACC and cerebellum and lesser connectivity of the CLR with M1F. These measures of functional brain connectivity could provide useful biomarkers to better understand human locomotor control and mechanisms of neurologic gait dysfunction, to assist with diagnosis, prognosis, and prescription of targeted neurobiology-based interventions.

ACKNOWLEDGMENTS

PB was supported by grant KL2TR001426 from the National Center for Advancing Translational Sciences at the National Institutes of Health, and by grant 17MCPRP33670446 from the American Heart Association. The authors declare no conflicts of interest.

ORCID

Pierce Boyne http://orcid.org/0000-0003-3611-9057

REFERENCES

Alam, M., Schwabe, K., & Krauss, J. K. (2011). The pedunculopontine nucleus area: Critical evaluation of interspecies differences relevant for its use as a target for deep brain stimulation. *Brain*, *134*, 11–23. https://doi.org/10.1093/brain/awq322

Allali, G., van der Meulen, M., Beauchet, O., Rieger, S. W., Vuilleumier, P., & Assal, F. (2014). The neural basis of age-related changes in motor imagery of gait: An fMRI study. *The Journals of Gerontology, Series A: Biological Sciences and Medical Sciences*, *69*, 1389–1398. https://doi.org/10.1093/gerona/glt207

Allen, G. I., & Tsukahara, N. (1974). Cerebrocerebellar communication systems. *Physiological Reviews*, *54*, 957–1006.

Armstrong, D. M. (1988). The supraspinal control of mammalian locomotion. *The Journal of Physiology*, *405*, 1–37.

ATS Committee on Proficiency Standards for Clinical Pulmonary Function Laboratories. (2002). ATS statement: Guidelines for the six-minute walk test. *American Journal of Respiratory and Critical Care Medicine*, *166*, 111–117.

Bakker, M., De Lange, F. P., Helmich, R. C., Scheeringa, R., Bloem, B. R., & Toni, I. (2008). Cerebral correlates of motor imagery of normal and precision gait. *NeuroImage*, *41*, 998–1010. https://doi.org/10.1016/j.neuroimage.2008.03.020

Bohannon, R. W., Horton, M. G., & Wikholm, J. B. (1991). Importance of four variables of walking to patients with stroke. *International Journal of Rehabilitation Research*, *14*, 246–250.

Bohnen, N. I., & Jahn, K. (2013). Imaging: What can it tell us about parkinsonian gait? *Movement Disorders*, *28*, 1492–1500. https://doi.org/10.1002/mds.25534

Brett, M., Johnsrude, I. S., & Owen, A. M. (2002). The problem of functional localization in the human brain. *Nature Reviews Neuroscience*, *3*, 243–249. https://doi.org/10.1038/nrn756

Buckner, R. L., Krienen, F. M., Castellanos, A., Diaz, J. C., & Yeo, B. T. (2011). The organization of the human cerebellum estimated by intrinsic functional connectivity. *Journal of Neurophysiology*, *106*, 2322–2345. https://doi.org/10.1152/jn.00339.2011

Coffman, K. A., Dum, R. P., & Strick, P. L. (2011). Cerebellar vermis is a target of projections from the motor areas in the cerebral cortex. *Proceedings of the National Academy of Sciences of the United States of America*, *108*, 16068–16073. https://doi.org/10.1073/pnas.1107904108

Cremers, J., D'Ostilio, K., Stamatakis, J., Delvaux, V., & Garraux, G. (2012). Brain activation pattern related to gait disturbances in Parkinson's disease. *Movement Disorders*, *27*, 1498–1505. https://doi.org/10.1002/mds.25139

Enright, P. L., & Sherrill, D. L. (1998). Reference equations for the six-minute walk in healthy adults. *American Journal of Respiratory and Critical Care Medicine*, *158*, 1384–1387.

Fan, L., Li, H., Zhuo, J., Zhang, Y., Wang, J., Chen, L., … Jiang, T. (2016). The human Brainnetome Atlas: A new brain atlas based on connectional architecture. *Cerebral Cortex*, *26*, 3508–3526. https://doi.org/10.1093/cercor/bhw157

Fasano, A., Laganiere, S. E., Lam, S., & Fox, M. D. (2017). Lesions causing freezing of gait localize to a cerebellar functional network. *Annals of Neurology*, *81*, 129–141. https://doi.org/10.1002/ana.24845

Finn, E. S., Shen, X., Scheinost, D., Rosenberg, M. D., Huang, J., Chun, M. M., … Constable, R. T. (2015). Functional connectome fingerprinting: Identifying individuals using patterns of brain connectivity. *Nature Neuroscience*, *18*, 1664–1671. https://doi.org/10.1038/nn.4135

Fling, B. W., Cohen, R. G., Mancini, M., Carpenter, S. D., Fair, D. A., Nutt, J. G., & Horak, F. B. (2014). Functional reorganization of the locomotor network in Parkinson patients with freezing of gait. *PLoS One*, *9*, e100291. https://doi.org/10.1371/journal.pone.0100291

Fling, B. W., Cohen, R. G., Mancini, M., Nutt, J. G., Fair, D. A., & Horak, F. B. (2013). Asymmetric pedunculopontine network connectivity in parkinsonian patients with freezing of gait. *Brain*, *136*, 2405–2418. https://doi.org/10.1093/brain/awt172

Fox, M. D., Buckner, R. L., Liu, H., Chakravarty, M. M., Lozano, A. M., & Pascual-Leone, A. (2014). Resting-state networks link invasive and noninvasive brain stimulation across diverse psychiatric and neurological diseases. *Proceedings of the National Academy of Sciences of the United States of America*, *111*, 4367. https://doi.org/10.1073/pnas.1405003111

Fox, M. D., & Greicius, M. (2010). Clinical applications of resting state functional connectivity. *Frontiers in Systems Neuroscience*, *4*, 19. https://doi.org/10.3389/fnsys.2010.00019

Fox, M. D., & Raichle, M. E. (2007). Spontaneous fluctuations in brain activity observed with functional magnetic resonance imaging. *Nature Reviews Neuroscience*, *8*, 700–711 doi: nrn2201[pii].

Gibbons, W. J., Fruchter, N., Sloan, S., & Levy, R. D. (2001). Reference values for a multiple repetition 6-minute walk test in healthy adults older than 20 years. *Journal of Cardiopulmonary Rehabilitation*, *21*, 87–93.

Godde, B., & Voelcker-Rehage, C. (2010). More automation and less cognitive control of imagined walking movements in high- versus low-fit older adults. *Frontiers in Aging Neuroscience*, *2*, 139. https://doi.org/10.3389/fnagi.2010.00139

Gwin, J. T., Gramann, K., Makeig, S., & Ferris, D. P. (2011). Electrocortical activity is coupled to gait cycle phase during treadmill walking. *NeuroImage*, *54*, 1289–1296. https://doi.org/10.1016/j.neuroimage.2010.08.066

Hanakawa, T., Fukuyama, H., Katsumi, Y., Honda, M., & Shibasaki, H. (1999). Enhanced lateral premotor activity during paradoxical gait in Parkinson's disease. *Annals of Neurology*, *45*, 329–336.

Holroyd, C. B., & Umemoto, A. (2016). The research domain criteria framework: The case for anterior cingulate cortex. *Neuroscience & Biobehavioral Reviews*, *71*, 418–443 doi:S0149-7634(16)30364-5[pii].

Iseki, K., Hanakawa, T., Shinozaki, J., Nankaku, M., & Fukuyama, H. (2008). Neural mechanisms involved in mental imagery and observation of gait. *NeuroImage*, *41*, 1021–1031. https://doi.org/10.1016/j.neuroimage.2008.03.010

Jaeger, L., Marchal-Crespo, L., Wolf, P., Luft, A. R., Riener, R., Michels, L., & Kollias, S. (2016). On the modulation of brain activation during simulated weight bearing in supine gait-like stepping. *Brain Topography*, *29*, 193–205. https://doi.org/10.1007/s10548-015-0441-7

Jaeger, L., Marchal-Crespo, L., Wolf, P., Riener, R., Michels, L., & Kollias, S. (2014). Brain activation associated with active and passive lower limb stepping. *Frontiers in Human Neuroscience*, *8*, 828. https://doi.org/10.3389/fnhum.2014.00828

Jahn, K., Deutschlander, A., Stephan, T., Kalla, R., Hufner, K., Wagner, J., … Brandt, T. (2008a). Supraspinal locomotor control in quadrupeds and humans. *Progress in Brain Research*, *171*, 353–362. https://doi.org/10.1016/S0079-6123(08)00652-3

Jahn, K., Deutschlander, A., Stephan, T., Kalla, R., Wiesmann, M., Strupp, M., & Brandt, T. (2008b). Imaging human supraspinal locomotor centers in brainstem and cerebellum. *NeuroImage*, *39*, 786–792 doi: S1053-8119(07)00880-4[pii].

Jahn, K., Deutschlander, A., Stephan, T., Strupp, M., Wiesmann, M., & Brandt, T. (2004). Brain activation patterns during imagined stance and locomotion in functional magnetic resonance imaging. *NeuroImage*, *22*, 1722–1731. https://doi.org/10.1016/j.neuroimage.2004.05.017

Jenkins, I. H., Jahanshahi, M., Jueptner, M., Passingham, R. E., & Brooks, D. J. (2000). Self-initiated versus externally triggered movements. II. The effect of movement predictability on regional cerebral blood flow. *Brain*, *123*(Pt 6), 1216–1228.

Jenkinson, M., Beckmann, C. F., Behrens, T. E., Woolrich, M. W., & Smith, S. M. (2012). FSL. *NeuroImage*, *62*, 782–790. https://doi.org/10.1016/j.neuroimage.2011.09.015

Karachi, C., Andre, A., Bertasi, E., Bardinet, E., Lehericy, S., & Bernard, F. A. (2012). Functional parcellation of the lateral mesencephalus. *The Journal of Neuroscience*, *32*, 9396–9401. https://doi.org/10.1523/JNEUROSCI.0509-12.2012

Karachi, C., Grabli, D., Bernard, F. A., Tande, D., Wattiez, N., Belaid, H., … Francois, C. (2010). Cholinergic mesencephalic neurons are involved in gait and postural disorders in Parkinson disease. *Journal of Clinical Investigation*, *120*, 2745–2754. https://doi.org/10.1172/JCI42642

Knaepen, K., Mierau, A., Tellez, H. F., Lefeber, D., & Meeusen, R. (2015). Temporal and spatial organization of gait-related electrocortical potentials. *Neuroscience Letters*, *599*, 75–80. https://doi.org/10.1016/j.neulet.2015.05.036

Kurz, M. J., Wilson, T. W., & Arpin, D. J. (2012). Stride-time variability and sensorimotor cortical activation during walking. *NeuroImage*, *59*, 1602–1607. https://doi.org/10.1016/j.neuroimage.2011.08.084

la Fougere, C., Zwergal, A., Rominger, A., Forster, S., Fesl, G., Dieterich, M., … Jahn, K. (2010). Real versus imagined locomotion: A [18F]-FDG PET-fMRI comparison. *NeuroImage*, *50*, 1589–1598. https://doi.org/10.1016/j.neuroimage.2009.12.060

Lancaster, J. L., Tordesillas-Gutierrez, D., Martinez, M., Salinas, F., Evans, A., Zilles, K., … Fox, P. T. (2007). Bias between MNI and Talairach coordinates analyzed using the ICBM-152 brain template. *Human Brain Mapping*, *28*, 1194–1205. https://doi.org/10.1002/hbm.20345

Martinez, M., Valencia, M., Vidorreta, M., Luis, E. O., Castellanos, G., Villagra, F., … Pastor, M. A. (2016). Trade-off between frequency and precision during stepping movements: Kinematic and BOLD brain activation patterns. *Human Brain Mapping*, *37*, 1722–1737. https://doi.org/10.1002/hbm.23131

Middleton, A., Fritz, S. L., & Lusardi, M. (2015). Walking speed: The functional vital sign. *Journal of Aging and Physical Activity*, *23*, 314–322. https://doi.org/10.1123/japa.2013-0236

Miyai, I., Tanabe, H. C., Sase, I., Eda, H., Oda, I., Konishi, I., … Kubota, K. (2001). Cortical mapping of gait in humans: A near-infrared spectroscopic topography study. *NeuroImage*, *14*, 1186–1192. https://doi.org/10.1006/nimg.2001.0905

Mori, S., Matsuyama, K., Mori, F., & Nakajima, K. (2001). Supraspinal sites that induce locomotion in the vertebrate central nervous system. *Advances in Neurology*, *87*, 25–40.

Muthusamy, K. A., Aravamuthan, B. R., Kringelbach, M. L., Jenkinson, N., Voets, N. L., Johansen-Berg, H., … Aziz, T. Z. (2007). Connectivity of the human pedunculopontine nucleus region and diffusion tensor imaging in surgical targeting. *Journal of Neurosurgery*, *107*, 814–820. https://doi.org/10.3171/JNS-07/10/0814

Nooner, K. B., Colcombe, S. J., Tobe, R. H., Mennes, M., Benedict, M. M., Moreno, A. L., … Milham, M. P. (2012). The NKI-Rockland sample: A model for accelerating the pace of discovery science in psychiatry. *Frontiers in Neuroscience*, *6*, 152. https://doi.org/10.3389/fnins.2012.00152

Perera, S., Mody, S. H., Woodman, R. C., & Studenski, S. A. (2006). Meaningful change and responsiveness in common physical performance measures in older adults. *Journal of the American Geriatrics Society*, *54*, 743–749 doi:JGS701 [pii].

Peterson, D. S., & Horak, F. B. (2016). Neural control of walking in people with parkinsonism. *Physiology (Bethesda)*, *31*, 95–107. https://doi.org/10.1152/physiol.00034.2015

Peterson, D. S., Pickett, K. A., Duncan, R., Perlmutter, J., & Earhart, G. M. (2014). Gait-related brain activity in people with Parkinson disease with freezing of gait. *PLoS One*, *9*, e90634. https://doi.org/10.1371/journal.pone.0090634

Power, J. D., Barnes, K. A., Snyder, A. Z., Schlaggar, B. L., & Petersen, S. E. (2012). Spurious but systematic correlations in functional connectivity MRI networks arise from subject motion. *NeuroImage*, *59*, 2142–2154. https://doi.org/10.1016/j.neuroimage.2011.10.018

Sebille, S. B., Belaid, H., Philippe, A. C., Andre, A., Lau, B., Francois, C., … Bardinet, E. (2017). Anatomical evidence for functional diversity in the mesencephalic locomotor region of primates. *NeuroImage*, *147*, 66–78 doi:S1053-8119(16)30719-4 [pii].

Shen, X., Tokoglu, F., Papademetris, X., & Constable, R. T. (2013). Groupwise whole-brain parcellation from resting-state fMRI data for network node identification. *NeuroImage*, *82*, 403–415. https://doi.org/10.1016/j.neuroimage.2013.05.081

Snijders, A. H., Leunissen, I., Bakker, M., Overeem, S., Helmich, R. C., Bloem, B. R., & Toni, I. (2011). Gait-related cerebral alterations in patients with Parkinson's disease with freezing of gait. *Brain*, *134*, 59–72. https://doi.org/10.1093/brain/awq324

Snijders, A. H., Takakusaki, K., Debu, B., Lozano, A. M., Krishna, V., Fasano, A., … Hallett, M. (2016). Physiology of freezing of gait. *Annals of Neurology*, *80*, 644–659. https://doi.org/10.1002/ana.24778

Takakusaki, K. (2013). Neurophysiology of gait: From the spinal cord to the frontal lobe. *Movement Disorders*, *28*, 1483–1491. https://doi.org/10.1002/mds.25669

Tian, Q., Chastan, N., Bair, W. N., Resnick, S. M., Ferrucci, L., & Studenski, S. A. (2017). The brain map of gait variability in aging, cognitive impairment and dementia-a systematic review. *Neuroscience & Biobehavioral Reviews*, *74*, 149–162 doi:S0149-7634(16)30484-5[pii].

Troosters, T., Gosselink, R., & Decramer, M. (1999). Six minute walking distance in healthy elderly subjects. *Eur Respir J*, *14*, 270–274.

Turkeltaub, P. E., Eickhoff, S. B., Laird, A. R., Fox, M., Wiener, M., & Fox, P. (2012). Minimizing within-experiment and within-group effects in Activation Likelihood Estimation meta-analyses. *Human Brain Mapping*, *33*, 1–13. https://doi.org/10.1002/hbm.21186

van der Meulen, M., Allali, G., Rieger, S. W., Assal, F., & Vuilleumier, P. (2014). The influence of individual motor imagery ability on cerebral recruitment during gait imagery. *Human Brain Mapping*, *35*, 455–470. https://doi.org/10.1002/hbm.22192

Wagner, J., Stephan, T., Kalla, R., Bruckmann, H., Strupp, M., Brandt, T., & Jahn, K. (2008). Mind the bend: Cerebral activations associated with mental imagery of walking along a curved path. *Experimental Brain Research*, *191*, 247–255. https://doi.org/10.1007/s00221-008-1520-8

Whitfield-Gabrieli, S., & Nieto-Castanon, A. (2012). Conn: A functional connectivity toolbox for correlated and anticorrelated brain networks. *Brain Connectivity*, *2*, 125–141. https://doi.org/10.1089/brain.2012.0073

Wilmore, J. H., Stanforth, P. R., Gagnon, J., Rice, T., Mandel, S., Leon, A. S., … Bouchard, C. (2001). Heart rate and blood pressure changes with endurance training: The HERITAGE family study. *Medicine & Science in Sports & Exercise*, *33*, 107–116.

Winkler, A. M., Ridgway, G. R., Webster, M. A., Smith, S. M., & Nichols, T. E. (2014). Permutation inference for the general linear model. *NeuroImage*, *92*, 381–397. https://doi.org/10.1016/j.neuroimage.2014.01.060

Winstein, C. J., Stein, J., Arena, R., Bates, B., Cherney, L. R., Cramer, S. C., … American Heart Association Stroke Council, Council on Cardiovascular and Stroke Nursing, Council on Clinical Cardiology, and Council on Quality of Care and Outcomes Research. (2016). Guidelines for adult stroke rehabilitation and recovery: A guideline for healthcare professionals from the American Heart Association/American Stroke Association. *Stroke*, *47*, e169. https://doi.org/10.1161/STR.0000000000000098

Wutte, M. G., Glasauer, S., Jahn, K., & Flanagin, V. L. (2012). Moving and being moved: Differences in cerebral activation during recollection of whole-body motion. *Behavioural Brain Research*, *227*, 21–29. https://doi.org/10.1016/j.bbr.2011.09.042

Yeo, B. T., Krienen, F. M., Sepulcre, J., Sabuncu, M. R., Lashkari, D., Hollinshead, M., … Buckner, R. L. (2011). The organization of the human cerebral cortex estimated by intrinsic functional connectivity. *Journal of Neurophysiology*, *106*, 1125–1165. https://doi.org/10.1152/jn.00338.2011

Yuan, J., Blumen, H. M., Verghese, J., & Holtzer, R. (2015). Functional connectivity associated with gait velocity during walking and walking-while-talking in aging: A resting-state fMRI study. *Human Brain Mapping*, *36*, 1484–1493. https://doi.org/10.1002/hbm.22717

Zwergal, A., Linn, J., Xiong, G., Brandt, T., Strupp, M., & Jahn, K. (2012). Aging of human supraspinal locomotor and postural control in fMRI. *Neurobiology of Aging*, *33*, 1073–1084. https://doi.org/10.1016/j.neurobiolaging.2010.09.022

SUPPORTING INFORMATION

Additional supporting information may be found online in the Supporting Information section at the end of the article.

How to cite this article: Boyne P, Maloney T, DiFrancesco M, et al. Resting-state functional connectivity of subcortical locomotor centers explains variance in walking capacity. *Hum Brain Mapp*. 2018;1–13. https://doi.org/10.1002/hbm.24326